An Improved Dictionary Design for Multicarrier Underwater Transmission

Xiang Huang and Rong-Rong Chen

***Abstract*—In this work, we study joint channel estimation and turbo equalization for coded orthogonal frequency division multiplexing (OFDM) in underwater acoustic (UWA) channels. We propose an alignment-aware basis (Aw-BS) design for compressed sensing (CS) based channel estimation that explicitly takes time-alignment of the OFDM blocks into account after Doppler resampling and carrier frequency offset (CFO) compensation. Using the data collected from actual underwater experiments, our results show that the proposed Aw-BS design enhances the CS algorithm's ability to focus on dominant signal paths, and yields superior performance to existing works that use a fixed basis for the CS based channel estimation.**

***Index Terms*—UWA, OFDM, compressed sensing, channel estimation, alignment, turbo equalization.**

I. Introduction

Underwater acoustic (UWA) channels are typically wideband due to the small ratio of the carrier frequency to the signal bandwidth, which introduces frequency-dependent Doppler shifts. Multi-carrier modulation in the form of orthogonal frequency-division multiplexing (OFDM) has been widely used for UWA communications. In [1], a novel two-stage approach is proposed to mitigate the Doppler effect for multicarrier communication over UWA channels. The two stages consists of a Doppler compensation via resampling, followed by a carrier frequency offset (CFO) compensation due to the residual Doppler. In [2], a compressed-sensing (CS) based channel estimation algorithm is developed to estimate the channel after the re-sampling and residual Doppler compensation. It is shown that the CS-based channel estimation can significantly outperform the conventional least squares (LS) channel estimation and achieve superior data detection performance in a turbo equalization setting.

The dictionary design in [2] adopts a fixed basis after the resampling and CFO compensation step, assuming that the time alignment of the OFDM blocks at the receiver side are perfect. We refer to this design as the fixed basis (Fx-BS) design. In actual transmissions, however, the alignment of the OFDM blocks needs to be estimated at the receiver, and the accuracy of the alignment often degrades as the mobility of the underwater vehicle increases. This motivates us to consider a new basis design that explicitly utilizes the time-alignment information. In this work, we propose an alignment-aware basis design (Aw-BS) using a newly derived discrete-time input and output channel model that incorporates the time alignment after resampling and CFO compensation. Our design directly applies discrete-time Fourier transformation (DFT) to determine the channel matrix, while the design in [2] is based on a continuous-time Fourier transformation. We note that a related design was examined in [3] but with single-carrier modulation and without turbo equalization. Using data from actual underwater experiments, we demonstrate the superior performance of the proposed Aw-BS design to the Fx-BS design under the setting of turbo equalization.

Xiang Huang and Rong-Rong Chen are with Dept. of ECE, University of Utah, USA. The work is supported in part by NSF grants CCF-1817154 and ECCS-1824558.

II. System Model Under Time Alignment

In the section, we introduce a new system model under time-alignment. While we follow the same zero-padded (ZP) OFDM modulation as in [2], our newly developed discrete-time system model incorporates several time-alignment parameters, which serves as a foundation for the proposed Aw-BS design discussed in Section III.

Assume each ZP-OFDM block duration is $T' = T + T_g$, where T_g is the zero guard interval and T is the OFDM symbol duration. The subcarrier spacing is $\triangle f = 1/T$. Let B denote the bandwidth and K the subcarrier number, where $B = K/T$. The passband signal of the w-th ZP-OFDM block is modeled as

$$\tilde{x}_w(t) = 2\mathrm{Re}\left\{ \left[\sum_{k=0}^{K-1} s_w[k] e^{j2\pi k \triangle f (t-t_w)} g(t-t_w) \right] e^{j2\pi f_c t} \right\} \tag{1}$$

where $t_w = wT'$, w is the index of ZP-OFDM block at a given time t (note that w starts from 0). From (1), we see that the transmitted w-th OFDM symbol corresponds to $t_w < t < t_w + T'$. The kth subcarrier is at frequency $f_k = f_c + k/T, \quad k = 0, \cdots, K-1$, f_c is the carrier frequency, and $s_w[k]$ is the symbol to be transmitted in the kth subcarrier of the w-th OFDM symbol. Let $\mathbf{s}_w = \mathbf{s}_w^p \cup \mathbf{s}_w^d \cup \mathbf{s}_w^n = [s_w[0], s_w[1], \cdots, s_w[K-1]]^T \in \mathbb{C}^{K\times 1}$. Here, $\mathbf{s}_w^p$, $\mathbf{s}_w^d$, and $\mathbf{s}_w^n$ respectively represent the sets of pilot subcarriers, data subcarriers, and null subcarriers. $g(t)$ is the rectangular function denoted as,

$$g(t) = \begin{cases} 1, & t \in [0, T] \\ 0, & \text{else} \end{cases} \tag{2}$$

We assume the UWA multipath channel has N_p discrete paths

$$h(\tau, t) = \sum_{p=1}^{N_p} A_p(t) \delta(\tau - (\tau_p - a_p t)) \tag{3}$$

where $A_p(t)$ and a_p are the amplitude and Doppler rate of the pth path, and τ_p is the delay at the start of the OFDM block. Hence, the simulated passband signal in the receiver is

$$\tilde{y}_w(t) = \sum_{p=1}^{N_p} A_p \tilde{x}_w((1+a_p)t - \tau_p) + \tilde{v}_w(t) \tag{4}$$

where $\tilde{v}_w(t)$ is the Gaussian noise. After applying the Doppler estimation method proposed in [1], we obtain the estimated Doppler $\hat{a}$. The resampling step, using the estimated Doppler

2023 57th Asilomar Conference on Signals, Systems, and Computers | 979-8-3503-2574-4/23/$31.00 ©2023 IEEE | DOI: 10.1109/IEEECONF59524.2023.10477070

$\hat{a}$, is then applied to the entire duration of the received signal. Subsequently, the carrier frequency offset (CFO) compensation is individually applied to each ZP-OFDM block, with distinctly estimated values of ε. After resampling, we will first determine the estimated CFO ε_w and the staring time $t_{0,w}$ for the w-th ZP-OFDM block during CFO compensation (a detailed description of the estimation of ε_w and $t_{0,w}$ is given at the end of this subsection). The resampled passband signal after CFO compensation is written as

$$\tilde{z}_w(t) = \tilde{y}_w(\frac{t}{1+\hat{a}})e^{-j2\pi\varepsilon_w t},\ t_{0,w}<t\leq t_{0,w}+\frac{(K+L)}{B} \tag{5}$$

By substituting Eq. (1) and (4) into Eq. (5), the resampled passband signal can be written as

$$\tilde{z}_w(t) = \Bigg(\sum_{p=1}^{N_p} A_p^* \Bigg[\sum_{k=0}^{K-1} s_w[k] e^{j2\pi k\triangle f((1+b_p)t-\tau_p-t_w)} g((1+b_p)t-\tau_p-t_w)\Bigg] e^{j2\pi f_c(1+b_p)t}\Bigg) e^{-j2\pi\varepsilon_w t} + \tilde{n}_w(t) \tag{6}$$

where $1+b_p = \frac{1+a_p}{1+\hat{a}}$, $A_p^* = A_p e^{-j2\pi f_c\tau_p}$ and $\tilde{n}_w(t)$ is the corresponding passband noise. The corresponding received baseband signal is then written as

$$z_w(t) = \sum_{p=1}^{N_p} A_p^* \Bigg(\Bigg[\sum_{k=0}^{K-1} s_w[k] e^{j2\pi k\triangle f((1+b_p)t-\tau_p-t_w)} g((1+b_p)t-\tau_p-t_w)\Bigg] e^{j2\pi f_c b_p t} e^{-j2\pi\varepsilon_w t}\Bigg) + n_w(t) \tag{7}$$

where $n_w(t)$ is the received baseband noise and $h_{p,w}(t) = g((1+b_p)t-\tau_p-t_w)$. The discrete-time baseband signal from Eq. (7) using the sampling period of $t_s = \frac{1}{B}$ is written as

$$z_w[nt_s] = \sum_{p=1}^{N_p} A_p^* \Bigg(\Bigg[\sum_{k=0}^{K-1} s_w[k] e^{j2\pi k\triangle f((1+b_p)nt_s-\tau_p-t_w)} h_{p,w}[nt_s]\Bigg] e^{j2\pi f_c b_p nt_s} e^{-j2\pi\varepsilon_w nt_s}\Bigg) + n_w[nt_s] \tag{8}$$

Efficient handling of the w-th baseband ZP-OFDM block signal requires alignment, necessitating the determination of the starting time $t_{0,w}$. To determine ε_w and $t_{0,w}$, we utilize a grid search for the optimal (ε, t_0), aiming to minimize the total power of null subcarriers in the w-th ZP-OFDM during CFO compensation. Here, ε is within the interval $[-2, 2]$ with a step size of 0.1. To ensure search accuracy, we consider the oversampling factor ρ, and assume that t_0 is within the interval $[t^i_{0,w} - \frac{2\rho}{B\rho}, t^i_{0,w} + \frac{2\rho}{B\rho}]$ with a step size of $\frac{1}{B\rho}$. The parameter $t^i_{0,w}$ denotes the initial starting time for the w-th ZP-OFDM block and is defined as $t^i_{0,w} = t_{0,w-1} + T'$. Note that relying solely on $t^i_{0,w}$ may not ensure obtaining a sufficiently small ε. Therefore, a fine search within a range centered at $t^i_{0,w}$ is necessary. To determine $t^i_{0,1}$, the first ZP-OFDM block is designated as the pilot block, allowing the utilization of correlation to refine the estimate for $t^i_{0,1}$.

III. Alignment-aware Basis Design

In this section, we present the proposed improved dictionary basis design. We first develop a discrete-time input-output model after resampling and CFO compensation. Based on this model, we then develop an improved dictionary basis design, which can achieve superior performance to the dictionary basis design of [2].

A. A New Dictionary Basis Design

We establish an input-output frequency domain relationship as $\mathbf{d}_w = \text{DFT}(\mathbf{z}_w) = \mathbf{H}_w\mathbf{s}_w + \mathbf{r}_w$, where $\mathbf{H}_w$ and $\mathbf{r}_w$ are channel and noise in frequency domain for the w-th ZP-OFDM block $\mathbf{z}_w$. Let $\mathbf{d}_w = [d_w[0], d_w[1], \cdots, d_w[K-1]]^T \in \mathbb{C}^{K\times 1}$. The frequency domain received signal at the m-th subcarrier from the w-th ZP-OFDM block is denoted as

$$d_w[m] = \frac{1}{K}\sum_{n=n_{0,w}}^{n_{0,w}+K+L-1} z_w[nt_s] e^{-j2\pi m\triangle f(n-n_{0,w})t_s} \tag{9}$$

where $n_{0,w} = \lfloor t_{0,w}/t_s \rfloor$ is the starting time index. By substituting Eq. (8) into Eq. (9), $d_w[m]$ can be written as Eqn. (10),

$$d_w[m] = \frac{1}{K}\sum_{n=n^1_{p,w}}^{n^2_{p,w}} \Bigg(\sum_{p=1}^{N_p} A_p^* \Bigg(\sum_{k=0}^{K-1} s_w[k] e^{j2\pi k\triangle f((1+b_p)nt_s-\tau_p-t_w)}\Bigg) e^{j2\pi(f_c b_p-\varepsilon_w)nt_s}\Bigg) e^{-j2\pi m\triangle f(n-n_{0,w})t_s} + r_w[m]. \tag{10}$$

where $n^1_{p,w}$ and $n^2_{p,w}$ represent the minimal and maximum integers of n for which the pulse shaping $h_{p,w}[n]$ have non-zero values for the w-th ZP-OFDM block. We note that computing $n_{0,w}$ does not necessitate knowledge of (b_p, τ_p), whereas determining $n^1_{p,w}$ and $n^2_{p,w}$ does requires this information. Subsequently, by changing the order of summation, we re-write $d_w[m]$ as

$$d_w[m] = \sum_{k=0}^{K-1} s_w[k]\Bigg[\sum_{p=1}^{N_p} A_p^*\Bigg(\frac{1}{K}\sum_{n=n^1_{p,w}}^{n^2_{p,w}} e^{j2\pi k\triangle f(1+b_p)nt_s} e^{j2\pi(f_c b_p-\varepsilon_w-m\triangle f)nt_s} e^{-j2\pi k\triangle f(\tau_p+t_w)} e^{j2\pi m\triangle f n_{0,w}t_s}\Bigg)\Bigg] + r_w[m]. \tag{11}$$

Based on Eq. (8), we determine $\mathbf{H}_w$ and the basis $\mathbf{\Lambda}^p_w$ as

$$\mathbf{H}_w[m,k] = \sum_{p=1}^{N_p} A_p^* \mathbf{\Lambda}^p_w[m,k], \tag{12}$$

$$\mathbf{\Lambda}^p_w[m,k] = \frac{1}{K}\sum_{n=n^1_{p,w}}^{n^2_{p,w}} e^{j2\pi k\triangle f(1+b_p)nt_s} e^{j2\pi(f_c b_p-\varepsilon_w-m\triangle f)nt_s} e^{-j2\pi k\triangle f(\tau_p+t_w)} e^{j2\pi m\triangle f n_{0,w}t_s}. \tag{13}$$

Let $B_k = e^{-j2\pi k\triangle f(\tau_p+t_w)}$, $B_m = e^{j2\pi m\triangle f n_{0,w}t_s}$, $C_k = e^{j2\pi k\triangle f(1+b_p)t_s}$ and $C_m = e^{j2\pi(f_c b_p-\varepsilon_w-m\triangle f)t_s}$, and the Eqn

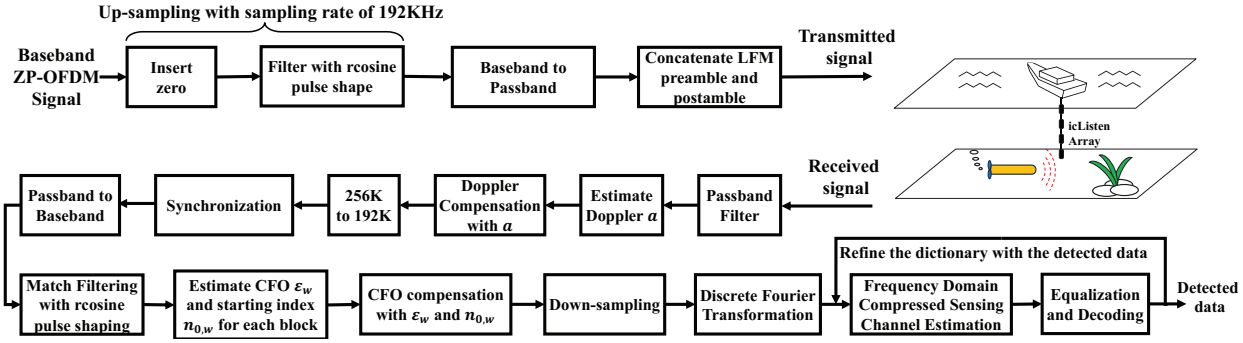

Fig. 1: The transmit and receive processing flowchart.

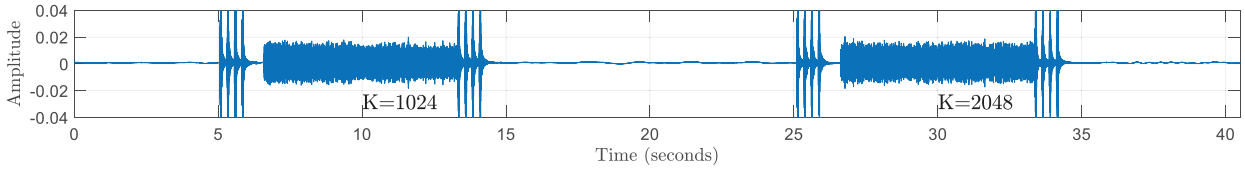

Fig. 2: Two received packets of $K = 1024$ and $K = 2048$

(13) can be expressed as

$$\begin{aligned}\mathbf{\Lambda}_w^p[m,k] &= \frac{B_m B_k}{K} \sum_{n=n_{p,w}^1}^{n_{p,w}^2} (C_k C_m)^n \\ &= \frac{B_m B_k}{K} \cdot \frac{(C_k C_m)^{n_{p,w}^1 - 1} - (C_k C_m)^{n_{p,w}^2}}{1 - C_k C_m}\end{aligned} \tag{14}$$

In contrast to the fixed basis in [2], our proposed basis $\mathbf{\Lambda}_w^p$ incorporates the alignment parameters $(n_{0,w}, n_{p,w}^1, n_{p,w}^2)$ to adapt to varying ZP-OFDM blocks. Both basis designs depend on the pairs of (b_p, τ_p). However, since the ground truth of pairs (b_p, τ_p) is unknown, the basis is designed based on the joint set of (b, τ),

$$\tau = \left\{ \frac{T}{\lambda K}, \frac{2T}{\lambda K}, \cdots, T_g \right\} \tag{15}$$

$$b = \{-b_{max}, b_{max} + \Delta b, \cdots, b_{max}\} \tag{16}$$

where we set the time resolution as $\frac{T}{\lambda K}$, and the Doppler rate resolution as Δb. λ is the factor to adjust the time resolution. Noticeably, The delay set τ has the size of $N_\tau = \lambda K T_g / T$, and the Doppler set b has the size of $N_b = 2b_{max}/\Delta b + 1$. There are total $N_\tau N_b$ paths to be searched, and the associated dictionary is $\mathbf{A}_w = [\mathbf{\Lambda}_w^1 \mathbf{s}_w, \cdots, \mathbf{\Lambda}_w^{N_\tau N_b} \mathbf{s}_w]$. We can re-write the input-output relationship as

$$\mathbf{d}_w = \underbrace{[\mathbf{\Lambda}_w^1 \mathbf{s}_w, ..., \mathbf{\Lambda}_w^{N_\tau N_p} \mathbf{s}_w]}_{\mathbf{A}_w} \begin{bmatrix} A_1^* \\ \vdots \\ A_{N_\tau N_p}^* \end{bmatrix} + \mathbf{r}_w \tag{17}$$

Due to the sparsity assumption of UWA channels, where $N_p \ll N_\tau N_b$, it becomes a ℓ_1 problem,

$$\min_{\mathbf{x} \in \mathbb{C}^n} \frac{1}{2} \|\mathbf{d}_w - \mathbf{A}_w \mathbf{x}\|_2^2 + \beta \|\mathbf{x}\|_1 \tag{18}$$

where $\mathbf{d}_w \in \mathbb{C}^{K \times 1}$, $\mathbf{A}_w \in \mathbb{C}^{K \times (N_\tau N_b)}$, $\mathbf{x} \in \mathbb{C}^{(N_\tau N_b) \times 1}$, $\tau \in \mathbb{R}^+$, $\|\cdot\|_2$ denotes the Euclidean mean, and $\|\cdot\|_1$ denotes the ℓ_1 norm. β is the sparsity factor. $\mathbf{x}$ is the estimated weight vector across $N_\tau N_b$ paths, in that $\mathbf{x} = [(\mathbf{x}^1), \cdots, (\mathbf{x}^{N_b})]^T$ and each $\mathbf{x}^i = [\xi_1^i, \cdots, \xi_{N_\tau}^i]$ is corresponding to all delays associated with the Doppler scale b_i. To solve this sparse estimation problem, especially in this complex number case, we use the SpaRSA algorithm based on iterative shrinkage/thresholding (IST) algorithm in [4].

IV. Turbo Receiver

In this section, we describe the key operations of the turbo receiver shown in Fig. 1 and highlight how the proposed Aw-BS CS channel estimation is integrated into the turbo loop.

After CFO compensation, we perform down-sampling on the baseband signal, followed by joint iterative channel estimation, equalization, and data decoding. At the first iteration, the dictionary $\mathbf{A}_w$ is generated using pilot symbols $\mathbf{s}_w^p$ only. Subsequently, the soft minimum mean square error (MMSE) equalizer [5] is applied to generate the extrinsic log-likelihood ratio (LLR) for the decoder. The decoder outputs the estimated symbols, contributing to the refinement of the dictionary $\mathbf{A}_w$ with $\mathbf{s}_w^p$ and the newly detected $\mathbf{s}_w^d$, in the subsequent iteration. Concurrently, the extrinsic LLR from the decoder serves as the *a priori* LLR for the soft MMSE equalizer in subsequent iterations. Through this iterative process of channel estimation and data detection, the accuracy of channel estimation is improved, leading to a reduction of error rates.

Furthermore, we employ maximum ratio combining (MRC) to enhance Signal-to-Noise Ratio (SNR). Assume n_r receive hydrophones are used. We can apply Aw-BS to estimate the channel seen by each hydrophone separately and let $\hat{\mathbf{H}}_w^n \in \mathbb{C}^{K \times K}$ denote the estimated channel for the w-th ZP-OFDM block using the n-th hydrophone. We then stack up received data from all n_r hydrophones to obtain a combined input-output relation in the frequency domain

$$\begin{bmatrix} \mathbf{d}_w^1 \\ \vdots \\ \mathbf{d}_w^{n_r} \end{bmatrix} = \begin{bmatrix} \hat{\mathbf{H}}_w^1 \\ \vdots \\ \hat{\mathbf{H}}_w^{n_r} \end{bmatrix} \mathbf{s}_w + \begin{bmatrix} \mathbf{r}_w^1 \\ \vdots \\ \mathbf{r}_w^{n_r} \end{bmatrix}. \tag{19}$$

TABLE I: Transmission parameters

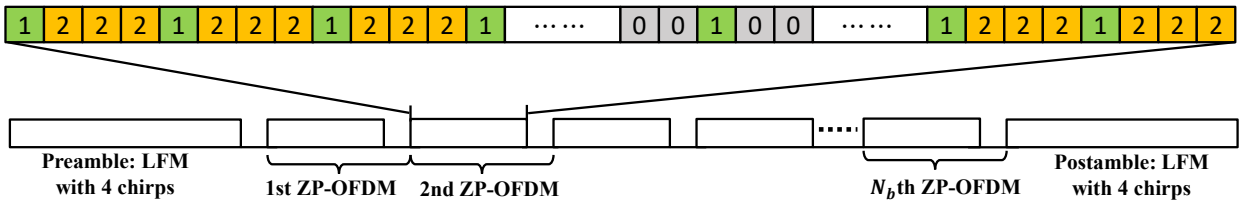

Fig. 3: OFDM subcarrier pattern in frequency domain. 0: null, 1: pilot, 2: data; Transmit format in time domain.

The soft MMSE equalizer operates based on (19) to jointly detect data symbols using signals received at all n_r hydrophones.

V. Description of Underwater Experiments

A field test was conducted at the lake of Tuscaloosa,

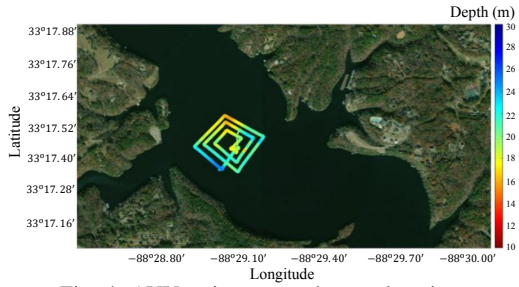

Fig. 4: AUV trajectory at the test location.

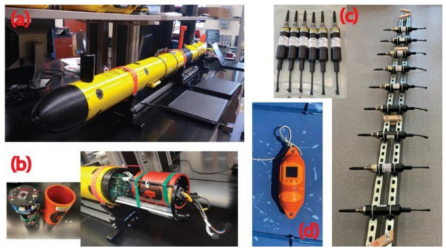

Fig. 5: Main instruments for field tests. (a) Mid-size AUV, EcoMapper. (b) Software-defined acoustic modem Subnero on the AUV. (c) Wideband digital hydrophones. (d) Handheld CTD. Figures are from NSF mu-Net. [6]

As shown in Tab. I, we use quadrature phase-shift keying (QPSK) as the modulation scheme. The signal has a carrier frequency f_c of 24 kHz and a bandwidth of 8 kHz. The lower sideband and upper sideband are 24 KHz and 32 KHz, respectively. The zero guard interval is 25 ms. Each orthogonal frequency-division multiplexing (OFDM) symbol consists of K subcarriers, which are divided into three types: pilot, null, and data. The pilot subcarriers are used for channel estimation, the null subcarriers are used for CFO compensation, and the data subcarriers are used for information transmission. The percentages of these subcarriers are 25%, 5.47%, and 69.53%, respectively. Fig. 3 shows the uniform distribution of the pilot subcarriers. We select 1.368% pilot subcarriers, each of which is surrounded by a group of four null subcarriers. These groups are also evenly spaced. The remaining subcarriers carry data. In transmission, we use (10, 20, 142, 2840, 1420) 5G quasi-cyclic (QC) binary LDPC code as the channel coding. Every two OFDM blocks carry one codeword for $K = 1024$, whereas, every OFDM block carries one codeword for $K = 2048$. We generate $N_b = 44$ and $N_b = 24$ basedband ZP-OFDM blocks for $K = 1024$ and $K = 2048$, respectively. As shown in Fig. 1, the basedband signal originally with the sampling rate of 8 KHz is then up-sampled with the oversampling factor of $\rho = 24$, to have the sampling rate of 192 KHz. After being carried to the carrier frequency of 24 KHz, we concatenate the preamble and postamble before and after the OFDM blocks. The linear frequency modulation (LFM) preamble and postamble occupy 1.5 secs each. Two received packets of $K = 1024$ and 2048 are shown in Fig. 2.

VI. Experimental Results

As depicted in Fig. 1, the received signal is captured using eight hydrophones. To eliminate extraneous noise beyond the passband, we initiate the process with a passband filter. Assuming a uniform Doppler shift across all eight received datasets, we choose one dataset to estimate the Doppler shift by comparing the reception durations between the Linear Frequency Modulation (LFM) chirps of the preamble and postamble with their original values before transmission.

Following this, we resample the filtered passband signal using the estimated Doppler shift $\hat{a}$ and adjust the sampling rate to 192 KHz, down from the original 256 KHz. After synchronization and downconversion from passband to baseband, we apply a matched filter with the same raised

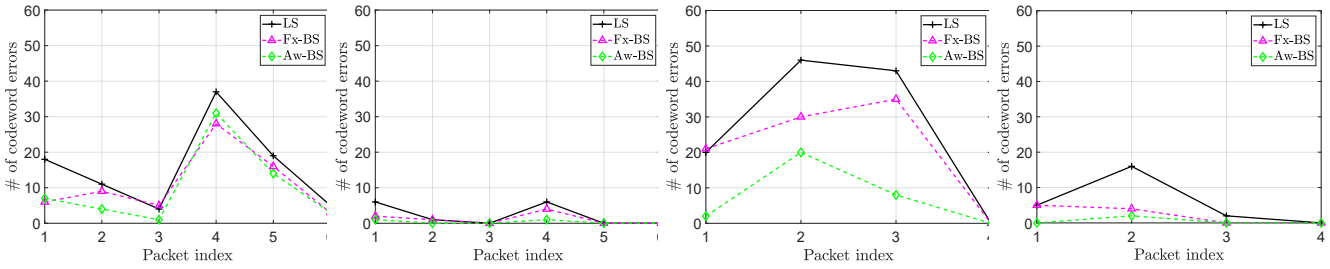

(a) 8 KHz, $K = 1024$, $n_r = 2$, (b) 8 KHz, $K = 1024$, $n_r = 3$ (c) 8 KHz, $K = 2048$, $n_r = 2$ (d) 8 KHz, $K = 2048$, $n_r = 3$

Fig. 6: Performance comparisons of LS, Fx-BS, and the proposed Aw-BS design.

cosine pulse shaping function utilized in the upsampling at the transmitter to improve the signal-to-noise ratio (SNR). Subsequently, CFO compensation is individually applied to each ZP-OFDM block, with the goal of minimizing the total power from null subcarriers. This is achieved by estimating CFO ε_w and the starting index $n_{0,w}$.

We selected 6 and 4 packets for in-depth analysis, corresponding to $K = 1024$ and $K = 2048$, respectively. Within each packet, a detailed examination is conducted on the subsequent 42 OFDM blocks for $K = 1024$ and 21 OFDM blocks for $K = 2048$. Since the first ZP-OFDM block is used as a pilot block, each packet yields 20 codewords available for thorough analysis. To augment our dataset, we utilize multiple receive hydrophones. The parameter n_r represents the number of receive hydrophones considered, and we explore scenarios with $n_r = 2$ and $n_r = 3$ receive datasets. By selecting three different combinations for each case, we have a total of 60 codewords available for analysis in each scenario. In the SpaRSA algorithm, we set the sparsity factor β to 2 and 5 for $K = 1024$ and $K = 2048$, respectively. The dictionary used in this study is only in the delay dimension (i.e. $b_{max} = 0$). We set the time resolution λ to 4. Fig. 6 provides a comparative analysis of the number of codeword errors achieved by our proposed basis design and other designs. In the figure, "LS" denotes the least square channel estimation, "Fx-BS" denotes the fixed basis design from [2], and "Aw-BS" denotes our proposed alignment-aware basis design. Fig. 7 shows exemplary time-domain channel impulse response (CIR) estimation from "LS", "Fx-BS", and "Aw-BS", when $K = 2048$ and $n_r = 2$. The following key observations summarize our findings.

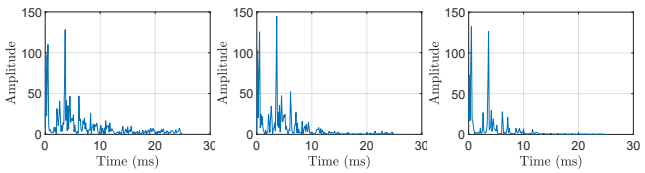

(a) "LS" (b) "Fx-BS" (c) "Aw-BS"

Fig. 7: CIR estimations from the 3rd packet of $K = 2048$ and $n_r = 2$

- The proposed basis design demonstrates superior performance for most scenarios. Notably, when $n_r = 3$, the improved SNR results in an error gap of less than 5 between the Aw-BS design and the Fx-BS design. In the case of $n_r = 2$, the error gap widens between the Aw-BS design and the Fx-BS design. This difference is significant in the third packet with $K = 2048$, where the gap reaches 27. This underscores the effectiveness of our proposed basis design, showing its ability to yield superior results under moderate SNR conditions and with smaller subcarrier spacing.
- Upon examining the CIR estimations depicted in Fig. 7 from LS, Fx-BS, and Aw-BS, the proposed design Aw-BS yields a sparser CIR estimation in comparison to Fx-BS design, while the LS approach produces the densest CIR estimation. This observation suggests that our proposed Aw-BS design enhances the CS algorithm's ability to focus on dominant signal paths, thereby contributing to a more precise and accurate channel estimation.

VII. Conclusion and Future Work

In this paper, we developed a new Aw-BS design for CS channel estimation in UWA OFDM communication. The new design can better capture the channel input and output relationship after resampling and CFO compensation. Using data collected from actual underwater experiments, we show that the proposed Aw-BS design provides superior performance to existing approaches that rely on a fixed basis. Directions for future work include testing of the proposed design using higher-order modulations and under higher mobility.

Acknowledgement

The authors would like to acknowledge NSF grants CNS-2016726 and CNS-2016582 and Dr. Aijun Song from the University of Alabama for supporting and conducting the underwater experiments used in this study.

References

[1] C. R. Berger, S. Zhou, J. C. Preisig, and P. Willett, "Sparse channel estimation for multicarrier underwater acoustic communication: From subspace methods to compressed sensing," *IEEE transactions on signal processing*, vol. 58, no. 3, pp. 1708–1721, 2009.

[2] J. Huang, S. Zhou, J. Huang, C. R. Berger, and P. Willett, "Progressive inter-carrier interference equalization for ofdm transmission over time-varying underwater acoustic channels," *IEEE Journal of Selected Topics in Signal Processing*, vol. 5, no. 8, pp. 1524–1536, 2011.

[3] F. Qu, X. Nie, and W. Xu, "A two-stage approach for the estimation of doubly spread acoustic channels," *IEEE Journal of Oceanic Engineering*, vol. 40, no. 1, pp. 131–143, 2014.

[4] S. J. Wright, R. D. Nowak, and M. A. Figueiredo, "Sparse reconstruction by separable approximation," *IEEE Transactions on signal processing*, vol. 57, no. 7, pp. 2479–2493, 2009.

[5] M. Tuchler, A. C. Singer, and R. Koetter, "Minimum mean squared error equalization using a priori information," *IEEE Transactions on Signal processing*, vol. 50, no. 3, pp. 673–683, 2002.

[6] A. Song, "Nsf mu-net: Shared infrastructure for mobile underwater networks (https://aquatictech.org/)."